

Northumbria Research Link

Citation: Workman, David, Hunter, Michael, Dover, Lynn and Tetard, David (2016) Synthesis of novel Iron(III) chelators based on triaza macrocycle backbone and 1-hydroxy-2(H)-pyridin-2-one coordinating groups and their evaluation as antimicrobial agents. *Journal of Inorganic Biochemistry*, 160. pp. 49-58. ISSN 0162-0134

Published by: Elsevier

URL: <http://dx.doi.org/10.1016/j.jinorgbio.2016.04.018>
<<http://dx.doi.org/10.1016/j.jinorgbio.2016.04.018>>

This version was downloaded from Northumbria Research Link: <http://nrl.northumbria.ac.uk/26767/>

Northumbria University has developed Northumbria Research Link (NRL) to enable users to access the University's research output. Copyright © and moral rights for items on NRL are retained by the individual author(s) and/or other copyright owners. Single copies of full items can be reproduced, displayed or performed, and given to third parties in any format or medium for personal research or study, educational, or not-for-profit purposes without prior permission or charge, provided the authors, title and full bibliographic details are given, as well as a hyperlink and/or URL to the original metadata page. The content must not be changed in any way. Full items must not be sold commercially in any format or medium without formal permission of the copyright holder. The full policy is available online: <http://nrl.northumbria.ac.uk/policies.html>

This document may differ from the final, published version of the research and has been made available online in accordance with publisher policies. To read and/or cite from the published version of the research, please visit the publisher's website (a subscription may be required.)



UniversityLibrary



Northumbria
University
NEWCASTLE



Synthesis of novel Iron(III) chelators based on triaza macrocycle backbone and 1-hydroxy-2(H)-pyridin-2-one coordinating groups and their evaluation as antimicrobial agents



David G. Workman, Michael Hunter, Lynn G. Dover, David Tétard*

Faculty of Health and Life Sciences, Northumbria University, Newcastle upon Tyne NE1 8ST, United Kingdom

ARTICLE INFO

Article history:

Received 14 December 2015
Received in revised form 4 April 2016
Accepted 12 April 2016
Available online 16 April 2016

Keywords:

Siderophore
Chelator
Biostatic agent
Bacterial growth
1-Hydroxy-2(1H)-pyridinone

ABSTRACT

Several novel chelators based on 1-hydroxy-2(1H)-pyridinone coordinating groups decorating a triaza macrocyclic backbone scaffold were synthesised as potential powerful Fe^{3+} chelators capable of competing with bacterial siderophores. In particular, a novel chloromethyl derivative of 1-hydroxy-2(1H)-pyridinone exploiting a novel protective group for this family of coordinating groups was developed. These are the first examples of hexadentate chelators based on 1-hydroxy-2(1H)-pyridinone to be shown to have a biostatic activity against a range of pathogenic bacteria. Their efficacy as biostatic agents was assessed revealing that minor variations in the structure of the chelator can affect efficacy profoundly. The minimal inhibitory concentrations of our best tested novel chelators approach or are comparable to those for 1,4,7-tris(3-hydroxy-6-methyl-2-pyridylmethyl)-1,4,7-triazacyclononane, the best Fe^{3+} chelator known to date. The retarding effect these chelators have on microbial growth suggests that they could have a potential application as a co-active alongside antibiotics in the fight against infections.

© 2016 The Authors. Published by Elsevier Inc. This is an open access article under the CC BY license (<http://creativecommons.org/licenses/by/4.0/>).

1. Introduction

Bacterial resistance to once effective antibiotics has emerged as a major health threat of the 21st century [1,2]. There is therefore an urgent need to develop new strategies to combat the spread of multi-drug resistant infections. One of the potential options currently being studied is the use of biostatic agents (i.e. inhibitors of bacterial growth) that could work synergistically with existing antibiotics and boost their efficacy [3–7]. Metal chelators can be used to that effect as their biostatic activity upon microorganisms has long been known. Their mode of action is thought to be the imposition of metal starvation on the microorganisms [8–10].

The $\text{Fe}^{3+}/\text{Fe}^{2+}$ redox couple is able to catalyse a broad range of biological reactions,[11] thus iron is an essential element ubiquitous to virtually all organisms, making it a desirable target for the prevention of microbial growth by chelation [12–15]. In the case of infections, the pathogen's source of iron is known to be the hosts themselves [16–18]. Although iron is plentiful, from the microbial perspective there is limited bioavailability; pathogenic bacteria use efficient iron acquisition mechanisms, often based on small molecules called siderophores [19]. Siderophores are predominantly hexadentate ferric chelators; their Fe^{3+} affinities/binding strengths can be very high and

thus they are able to acquire otherwise unavailable iron from sequestered host sources [20–24]. Achieving a biostatic effect by iron starvation therefore appears to depend upon a deceptively simple thermodynamic and kinetic competition in the binding of Fe^{3+} cations by the bacterial siderophores and the added chelator. Alongside the difficult design of chelators that can compete effectively with siderophores, great care must also be taken to avoid toxic demetallation of host metalloenzymes, making development of this technology a non-trivial matter.

To compete with strong siderophores, the right choice of coordinating groups is crucial. When considering only the thermodynamic competition between bacterial siderophores and an added chelator, one must primarily consider the respective pFe^{3+} values (defined as $-\log[\text{Fe}^{3+}]_{\text{free}}$, usually calculated at pH 7.4, with $[\text{Chelator}]_{\text{total}} = 10 \mu\text{M}$ and $[\text{Fe}^{3+}]_{\text{total}} = 1 \mu\text{M}$ and cited herein in these conditions) of the two chelators to estimate which is most likely to be potent in complexing the metal [25]. It would appear that three isomers of the hydroxypyridinone (HOPO) family (Fig. 1) possess the right combination of pKa and $\log\beta(\text{Fe}^{3+})$ to give high pFe^{3+} values and therefore thermodynamically compete with siderophores (that are commonly based on coordinating groups such as α -hydroxycarboxylic acids, hydroxamic acids and catechols) [24,26].

These hydroxypyridinones also offer attractive additional prospects. Many bacteria can use siderophores elaborated by those of another species [18,27]; to be effective biostatic agents, synthetic chelators must not suffer from this “siderophore piracy” and actually promote bacterial

* Corresponding author.

E-mail address: david.tetard@northumbria.ac.uk (D. Tétard).

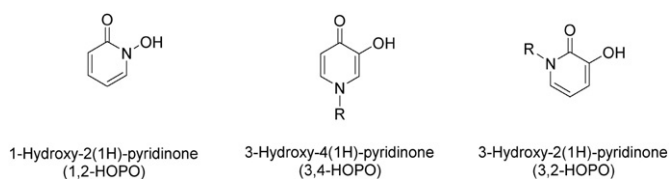


Fig. 1. Three relevant isomers of the HOPO family.

growth. Because very few HOPO are found in nature and only one has been described as a siderophore ligand (1-hydroxy-5-methoxy-6-methyl-2(1H)-pyridinone also called cepabactin), the likelihood of the metallated chelators being recognised by bacterial receptors and used as a source of Fe^{3+} is expected to be small. Additionally, infected human hosts are known to use various Fe^{3+} withholding strategies to limit bacterial growth. One of these is based on the activity of siderocalin, a protein that in essence acts as a trap for some siderophores [28–31]. A therapeutic chelator must not interact with siderocalin and inhibits its protective action. It is known that some 1-hydroxy-2(1H)-pyridinone (1,2-HOPO) based chelators do not bind strongly to siderocalin, suggesting that this class of coordinating groups would complement rather than overwhelm this defence strategy [32].

Members of the 3-hydroxy-4(1H)-pyridinone (3,4-HOPO) sub-family have been extensively studied in chelation therapies [33]. A significant number of reports have also described growth inhibition of a range of pathogenic bacteria by bidentate or hexadentate chelators based upon 3,4-HOPO [34–43]. To achieve high pFe^{3+} , hexadentate chelators are preferred to bidentate ones, especially since their mode of action as biostatic agents is expected to be extracellular and therefore do not suffer from size restriction to penetrate the microbes. A very small number of compounds belonging to the 1,2-HOPO sub-family were described as antimicrobial agents [44,45] but these are all bidentate chelators. No hexadentate member of that 1,2-HOPO sub-family has been described as antimicrobial agent. This absence of reports is surprising considering that a few hexadentate chelators based on 1,2-HOPO were described (for complexation of non-biologically relevant metals) whose structural features and chelation properties make them attractive candidates for this purpose (for example compounds **1** and **2**, Fig. 2) [46–49]. Although slightly weaker coordinating groups than their 3-hydroxy-2(1H)-pyridinone (3,2-HOPO) and 3,4-HOPO isomers, 1,2-HOPO coordinating groups possess another advantage that make them more attractive than their isomers. Their lower pK_a values (typically 6 versus 8.5–10 depending on substitution [26]) make them charged molecules at physiological pH and therefore less likely to

penetrate cells of the host. This could have beneficial safety benefits in treating systemic infections.

Although not based on HOPO, compound **3** has the highest known value of pFe^{3+} (see below) and is therefore expected to be able to compete favourably with siderophores for ferric cations at low concentration and therefore show high biostatic efficacy [50]. Despite its high pFe^{3+} value, to the best of our knowledge this compound has never been described as a biostatic agent. It was therefore considered necessary to synthesise, screen and use compound **3** as a benchmark.

Our interest in developing powerful Fe^{3+} -optimised chelators as biostatic agents prompted us to investigate a range of hexadentate chelators based on 1,2-HOPO and a triaza macrocyclic backbone scaffold to try to identify novel microbiostatic chelators. Very few polyaza macrocycles bearing HOPO coordinating groups have been described [48,51–54]. Macrocycles offer the potential to fine tune the metal chelating properties by varying the cycle's size and flexibility. Our aim was to combine key structural elements of siderophores, HOPO and 1,4,7-tris(3-hydroxy-6-methyl-2-pyridylmethyl)-1,4,7-triazacyclononane (TACN-MeHP, **3**) into a novel series of chelators. In particular by analogy with enterobactin (Fig. 3, compound **4**), it is speculated that the effect of the macrocyclic backbone scaffold could be beneficial to the efficacy of metal binding and therefore to the minimum inhibitory concentration (MIC) of the chelator. Moreover, no previous synthesis of hexadentate chelators where 1,2-HOPO moieties were linked to the molecular scaffold via a methylene bridge were ever reported, the focus having been on a carbonyl linker. The impact of that linker on metal chelation efficacy can be dramatic and therefore deserves in-depth study. Reported herein is the synthesis of novel triaza macrocyclic chelators bearing 1,2-HOPO moieties, linked via methylene or carbonyl groups and the study of their biostatic effect on a range of microorganisms, including a comparison with that of known compounds **1–3**.

2. Results and discussion

2.1. Organic synthesis

Our chelator design has focused on thermodynamic (pFe^{3+}) rather than kinetic considerations. One of the most remarkable bacterial siderophores is enterobactin (**4**), whose scaffold is composed of a triserine macrocycle (Fig. 3), and has been extensively studied owing to its very powerful Fe^{3+} chelation ($\log\beta_{110} = 49$ and $\text{pFe}^{3+} = 34.3$, where β_{mlh} is defined as the equilibrium constant for the reaction $\text{L} + \text{m M} + \text{h H}^+ \rightleftharpoons \text{L}_m\text{M}_h\text{H}_h$ [25]) [55]. The origin of its efficient binding has been elucidated and shown to be influenced by the pre-organisation

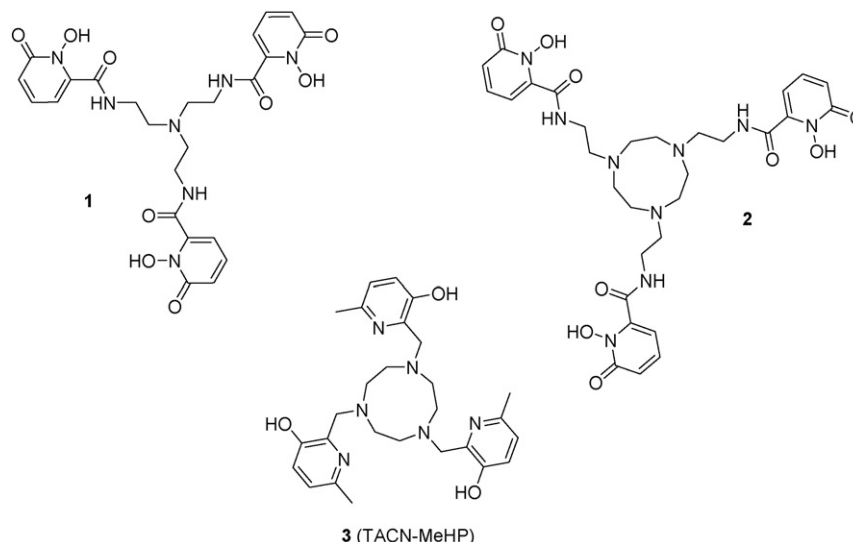


Fig. 2. Examples of known hexadentate chelators based on 1,2-HOPO (**1**, **2**) and 1,4,7-tris(3-hydroxy-6-methyl-2-pyridylmethyl)-1,4,7-triazacyclononane (TACN-MeHP) (**3**).

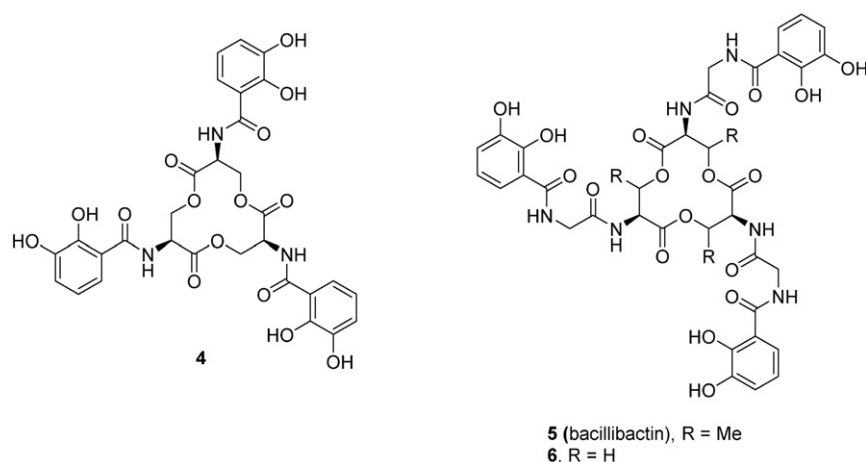


Fig. 3. Structure of siderophores enterobactin (4), bacillibactin (5) and synthetic analogue 6.

of the coordinating groups, itself largely influenced by the cyclic structure of its scaffold and intra-molecular hydrogen bonding [55–59]. Interestingly, bacillibactin (5), a siderophore analogue of enterobactin with glycine spacers linked to a tris-threonine macrocyclic scaffold also shows large $\log\beta_{110}$ and pFe^{3+} values (47.6, 33.1 respectively) [55]. However, synthetic analogue 6, also composed of a glycine spacer but of a tris-serine scaffold has poorer $\log\beta_{110}$ and pFe^{3+} values (44.1 and 29.6 respectively). It would appear that the nature of the spacer and the nature of the scaffold have a profound impact on pFe^{3+} that we hypothesise as having a key influence on growth inhibition.

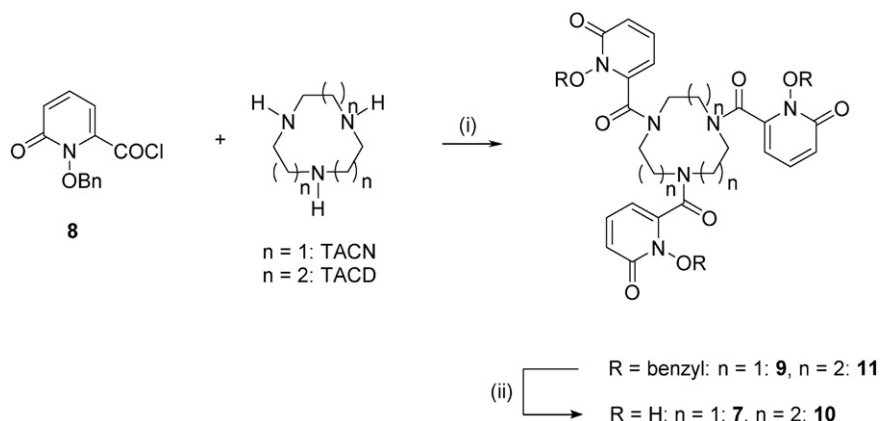
Compound 3 has a Fe^{3+} coordination environment in complexes that is very different to that of enterobactin or HOPO-based hexadentate chelators. Contrary to the O6 donor set of 1, 2, 4, the coordination of 3 on Fe^{3+} occurs through an N3O3 donor set involving the three nitrogen atoms of the 1,4,7-triazacyclononane (TACN) ring. As mentioned earlier, 3 has the highest known $\log\beta_{110}$ and the highest pFe^{3+} values of any known ligand ($\log\beta_{110} = 49.98$, $pFe^{3+} = 39.4$) and therefore is also worthy of consideration as a potential template to improve metal chelating ability of the molecules [50]. Although Fe^{3+} coordination studies with hexadentate analogues with a larger triaza macrocyclic cores were not fully described, it would appear that the three nitrogen atoms are sensibly at the right distance to efficiently bind the metal atom.

Inspired by these observations, and wanting to study a range of chelators based on 1,2-HOPO and bearing structural similarities to compounds 1–3 we first synthesised compound 7 from TACN as depicted in Scheme 1.

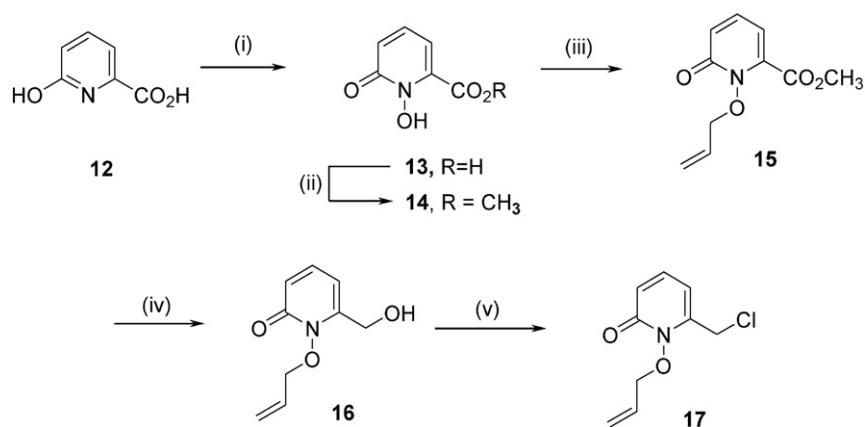
The first step in the preparation of 7 was performed based upon an existing procedure by reacting known acyl chloride 8 with TACN in THF [60]. Protected chelator 9 was obtained in low yield (25%). Removal

of the benzyl groups from 9 using a mixture of concentrated hydrochloric and glacial acetic acid yielded 7 in excellent yield (97%). An analogue of that compound with the larger triaza macrocycle (i.e. 1,5,9-triazacyclododecane, TACD) was also synthesised to allow for comparison of the effect of the ring size upon bacterial growth inhibition (Scheme 1). Reaction of acyl chloride 8 with TACD in DMF allowed for the isolation of the larger core protected molecule 11 in 49% yield. A similar acid deprotection gave 10 in good yield (71%).

It was anticipated that the amide linkage used in 7 and 10 would have a large impact on the conformational flexibility of the chelator [61] and also possibly an electronic effect on the 1,2-HOPO coordinating groups. That in turn could have an important impact (either beneficial or detrimental) on Fe^{3+} binding but the exact effect of these linkers is still unreported. Therefore, we also investigated the synthesis of an analogue of 7, replacing the carbonyl groups with methylene units. A novel HOPO protection strategy away from the benzyloxy protection traditionally used for 1,2-HOPO would be required. Indeed, it was predicted that benzyl protection would not be suitable as the most common methods used for its removal could also cleave the linkage between our HOPO group and the molecular backbone. Of the potential protective methods identified, protection of the *N*-hydroxyl group as the allyloxy group was undertaken. It was considered that deprotection can be afforded under a range of relatively mild conditions by double bond isomerisation and subsequent hydrolysis without compromising other bonds in the chelator [62]. The key allyl protected 6-hydroxymethyl intermediate 17 was synthesised in five steps from commercially available 12 (Scheme 2) [63]. This hydroxymethyl derivative could then be converted to the novel chloromethyl derivative 17 by thionyl chloride for incorporation onto ligand cores.



Scheme 1. Reagents and conditions: $n = 1$: (i) TACN, NEt_3 , THF, 60 °C; 25% (ii) HCl: AcOH; 97%; $n = 2$: (i) TACD, NEt_3 , DMF, 60 °C; 49% (ii) HCl: AcOH; 71%.



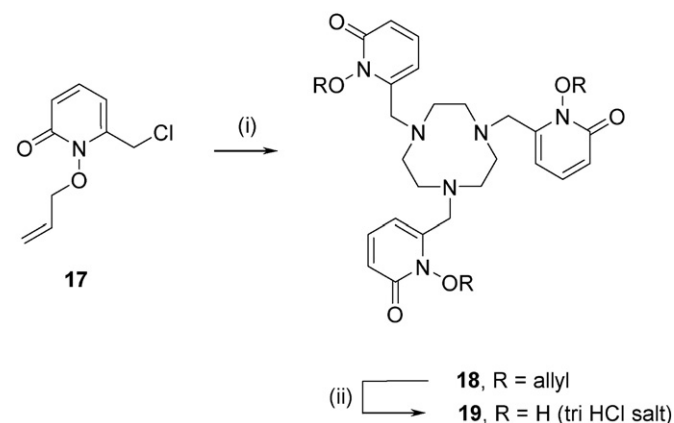
Scheme 2. Reagents and conditions: (i) $\text{CH}_3\text{CO}_3\text{H}$, AcOH , 80°C ; 77% (ii) MeOH , SOCl_2 , reflux; 96% (iii) $\text{CH}_2\text{CHCH}_2\text{Br}$, K_2CO_3 , acetonitrile, reflux; 94% (iv) NaBH_4 , MeOH , THF , reflux; 65% (v) SOCl_2 , CH_2Cl_2 , reflux; 92%.

Oxidation to the expensive 1.2-HOPO-6-carboxylate **12** was performed using commercially available peroxyacetic acid, a modification to the existing procedure of Xu et al. [60], resulting in a slightly increased yield (77%) without the use of also expensive trifluoroacetic acid. Treatment of the free acid **13** with thionyl chloride in methanol, following the method of Burgada et al. [64], gave the methyl ester **14** in excellent yield (96%). Subsequent protection of the *N*-hydroxyl group, using allyl bromide and potassium carbonate, yielded the novel methyl ester **15** (94%). Reduction of the ester **15** to the methyl alcohol **16** was accomplished by slow addition of methanol to sodium borohydride in THF, remarkably without reduction of the allyl group [65,66]. Notably, most of these steps gave acceptable to excellent yields. Workup of the reaction mixtures were easy to perform and the products either needed no purification at all or were easy to purify.

Reaction of a stoichiometric quantity of **17** with TACN in the presence of potassium carbonate produced the allyl protected macrocyclic product **18** in a yield of 93% (Scheme 3). The removal of the allyl protective group was performed using boron trichloride, without cleavage of the newly formed C–N bond, to give compound **19** as the said analogue of **7**. To the best of our knowledge, compound **19** is the first example of a 1.2-HOPO metal chelator anchored to its scaffold via a methylene link in position 6.

Finally, in order to discern any correlation of scaffold rigidity and biostatic effect, the acyl chloride intermediate **8** was also reacted with diethylenetriamine, a linear analogue of the cyclic TACN, to give chelator **20** after acid deprotection (Scheme 4).

Although chelators **1–3** were previously described in the literature they have not been evaluated as biostatic agents therefore their



Scheme 3. Reagents and conditions: (i) TACN, K_2CO_3 , CH_3CN , reflux; 93% (ii) BCl_3 , CH_2Cl_2 ; 87%.

synthesis was also undertaken in order to assess their antimicrobial properties [48,49,67].

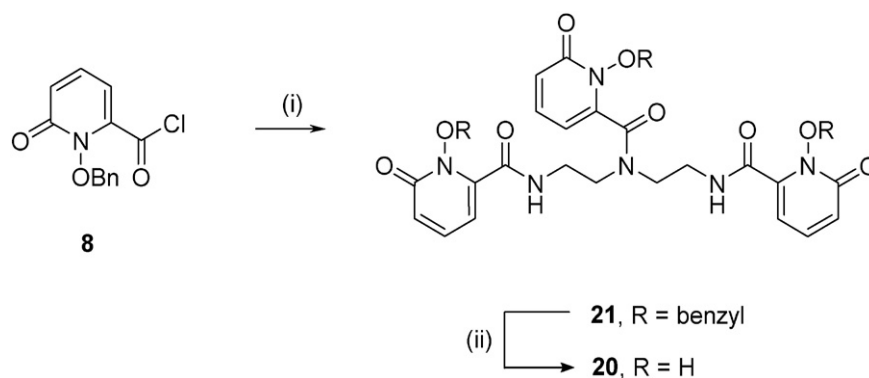
Chelator **19** was considered to be an interesting compound in several respects. One of them concerns the way in which it can chelate Fe^{3+} . The typical mode of coordination of 1.2-HOPO-based hexadentate chelators on trivalent metals such as Fe^{3+} and Ga^{3+} is via the two oxygen atoms (Fig. 4A), giving an O_6 coordination environment [32]. By analogy with derivatives of TACN-HP [68,69] but more importantly with a ligand closely related to **19**, i.e. a TACN-based tris-hydroxypyranone ligand 1,4,7-tris(3-hydroxy-6-(hydroxymethyl)-4(1*H*)-pyranon-2-ylmethyl)-1,4,7-triazacyclononane (NOKA) [70], it is possible to consider another mode of Fe^{3+} chelation, via a N_3O_3 coordination mode involving the TACN backbone and hydroxyl groups (Fig. 4B).

To further study the exact coordination mode of ligand **19**, in particular by NMR, Ga^{3+} was used as a surrogate for Fe^{3+} [71]. No in-depth study by MS or NMR of 1.2-HOPO based complexes of Ga(III) exist in the literature. For example, only one derivative of 1.2-HOPO complex (based on the 1-oxo-2-hydroxy-isoquinoline-3-carboxylic acid) of Ga(III) has been characterised by NMR in CDCl_3 [72]. Critically, no study of the chelation by NMR or MS was performed in water, a solvent more relevant to our growth media and where protonation reactions can have a dramatic impact on the species formed [73]. To try and establish spectroscopic features that would allow us to distinguish an N_3O_3 from an O_6 coordination mode, we were forced to first investigate by MS and NMR the complexation of Ga(III) on a model system. Compound **22** that we described for another type of application has been selected as such a model of ligand **19** [63].

It was judged that compound **22** in the presence of Ga(III) would form a 3:1 complex via the six oxygen atoms of three 1.2-HOPO bidentate ligands (Fig. 5). Therefore, compound **23** would be a good model of the coordination environment around Ga(III) if ligand **19** coordinated Ga(III) in a O_6 mode (Fig. 4A) and by extension, would give us some information on the way Fe^{3+} is chelated by **19**.

Proton and carbon NMR were first performed on solutions of **22** and **19** in D_2O . To these solutions, a stoichiometric amount of $\text{Ga}(\text{acac})_3$ (acac = acetylacetonate) was then added and the solutions incubated at room temperature for 24 h. The ^1H and ^{13}C NMR of the resulting complexes were then recorded. Also, these solutions, after dilution with methanol (non-deuterated), were analysed by MS.

Starting with MS, **22** + $\text{Ga}(\text{acac})_3$ (3:1 molar ratio) gave major peaks that match (m/z values and isotopic distribution) the formula $[(\mathbf{22} - 3\text{H})\text{Ga} + \text{Na}]^+$ at m/z 511.93 (expected 512.02), 512.93 (expected 513.02), 513.93 (expected 514.02), 515.00 (expected 515.02) and 516.00 (expected 516.02) (Fig. S1), confirming the displacement of the three acac ligands and strongly suggesting the formation of the 3:1 complex **23** as expected.



Scheme 4. Reagents and conditions: (i) diethylenetriamine, NEt₃, THF, 60 °C; 91% (ii) HCl: AcOH; 70%.

The MS of **19** + Ga(acac)₃ (1:1 molar ratio) gave major peaks that match (*m/z* values and isotopic distribution) the formula [(**19** – 3H)Ga + H]⁺ at *m/z* 565.13 (expected 565.13), 566.13 (expected 566.13), 567.13 (expected 567.13), 568.13 (expected 568.13) and 569.07 (expected 569.13) (Fig. S2). This result confirms that ligand **19** is capable of displacing the three acac ligands and that formation of a 1:1 complex occurred and that these involve the deprotonation of the three hydroxyl groups. This result cannot allow us to differentiate between the two coordination modes mentioned above.

In NMR, we expected that coordination of the HOPO moiety to Ga(III) would result in distinct changes to the chemical shifts of key protons and/or carbon atoms of the ligand and it was anticipated that these could be characteristic of the two coordination modes. The ¹H and ¹³C NMR spectra are given in Figs. S3 and S4 respectively. The ¹H of ligand **22** in D₂O in the absence or presence of 1/3 molar equivalent of Ga(acac)₃ indicated that upon complexation, the three signals of the 1,2-HOPO group are shifted downfield by no more than 0.3 ppm. The ¹H NMR of **19** + Ga(acac)₃ also showed a downfield shift of the chemical shifts but by a larger value of 0.6 ppm. These differences could suggest a different coordination mode. The presence of only one set of slightly broadened signals for the 1,2-HOPO moiety in the case of **19** + Ga(acac)₃ indicates that they are all largely equivalent and therefore all similarly coordinating, as suggested by the mass spectrum. The signals for the TACN scaffold are much more impacted by the presence of the metal. Instead of well-defined singlet in the ligand, various broad signals are seen between 3.1 and 4.1 ppm. Appearance of broad signals for In(III) complexes of NOKA has been observed at elevated temperature (contrary to the Ga(III)NOKA complex where the signals remained as well defined multiplets even at 85 °C) [70]. This has been ascribed to rapid exchange between the Δ and Λ isomers. The broad signals observed in our complex suggest that this rapid exchange exist even at room temperature.

In the ¹³C spectrum of **22** with and without Ga(acac)₃, the signal assigned to the carbon atom of the carbonyl is also shifted, upfield this time by 3.3 ppm. Interestingly, the most impacted signals correspond to the three C–H groups. The ¹³C NMR of **19** + Ga(acac)₃ is drastically different from that of the parent ligand and that of the analogous

complex **23**. Again, focusing on the signals for the TACN's methylene group, several signals are now seen, confirming the distorted nature of the scaffold. The signals associated with the carbon atoms in the 1,2-HOPO groups are also drastically shifted upon complexation. For example, one signal was found at 195.4 ppm corresponding to a quaternary carbon atom that did not appear in the spectrum of the free ligand. The differences between the ¹H and ¹³C NMR of **19** and **22** with and without Ga(III) suggest that the two ligands provide a different coordination mode. Because **22** is expected to provide an O₆ coordination environment, we tentatively suggest that an N₃O₃ coordination mode exists for ligand **19** + Ga(III) and therefore by extension to **19** + Fe(III) but further work will be necessary to draw a firmer conclusion.

2.2. Biostatic activity

We selected a small panel of diverse microbes to assess the efficacy of these chelators; these included bacteria from both Gram negative and Gram positive lineages as well as the pathogenic dimorphic fungus *Candida albicans*. Some species were selected for their implication in healthcare-associated infections, where possible strains previously used in the assessment of iron chelators or pharmaceuticals were used. *Bacillus subtilis* strain DSM-23,778 lacks a key phosphopantetheinyl transferase activity [74] required for siderophore biosynthesis and generates the bidentate itoic acid rather than the hexadentate bacillibactin [75]. Broth microdilution tests were undertaken based upon a standard procedure [76]. The results obtained are shown in Table 1. The commercially available *N,N,N',N',N''*-diethylenetriaminepentaacetic acid (DTPA) was also assayed for comparison purposes.

Across the range of microorganisms tested, it would appear that compounds **1** and **3** are systematically the best inhibitors of microbial growth (supplementary material, Table S). Compound **19** also appears to be one of the better chelators but it failed to equal the former

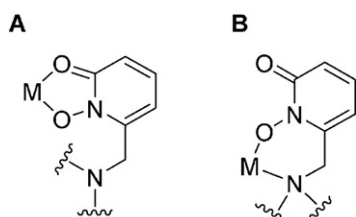


Fig. 4. Possible coordination modes for compound **19** with trivalent metal M (e.g. Fe³⁺, Ga³⁺).

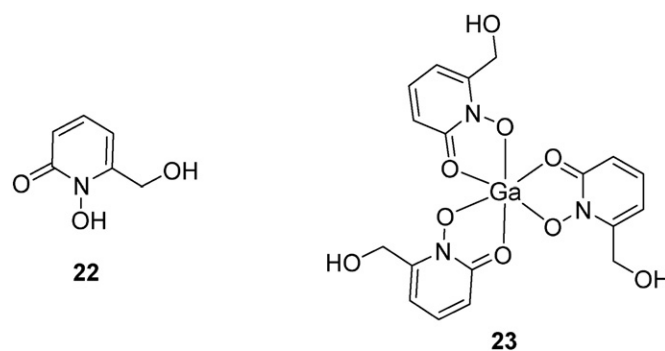


Fig. 5. 6-hydroxymethyl-1-hydroxy-2(1H)-pyridinone (**22**) and its expected 3:1 complex with Ga(III) (**23**).

Table 1
Minimum Inhibitory Concentrations (MIC) expressed in μM (in mg/L between brackets) for the ligands tested upon a panel of microorganisms. Results were determined in triplicate. The molar mass (g/mol) of each chelator is given between brackets in the first column.

Chelator (molar mass/g/mol)	Minimum Inhibitory Concentration/ μM (mg/L)						
	<i>E. coli</i> DSM-18039	<i>K. pneumoniae</i> DSM-30104	<i>P. aeruginosa</i> DSM-19880	<i>A. baumannii</i> DSM-30007	<i>B. subtilis</i> DSM-23778	<i>S. aureus</i> DSM-1104	<i>C. albicans</i> DSM-1386
DTPA (393.35)	2542 (1000)	2542 (1000)	>2542 (> 1000)	2542 (1000)	159 (62.5)	79 (31.1)	318 (125.1)
1 (557.52)	625 (348.5)	313 (174.5)	313 (174.5)	313 (174.5)	313 (174.5)	5 (2.8)	313 (174.5)
2 (669.70)	5000 (3348)	5000 (3348)	5000 (3348)	1250 (837.1)	313 (209.6)	625 (418.6)	78 (52.2)
3 (492.63)	78 (38.4)	313 (154.2)	625 (307.9)	156 (76.9)	78 (38.4)	78 (38.4)	39 (19.2)
7 (537.60)	5000 (2688)	>5000 (>2688)	5000 (2688)	5000 (2688)	5000 (2688)	2500 (1344)	313 (168.3)
10 (576.66)	5000 (2883)	5000 (2883)	2500 (1442)	313 (180.5)	1250 (720.8)	625 (360.4)	39 (22.5)
19 (492.63)	625 (307.9)	1250 (615.8)	625 (307.9)	313 (154.2)	313 (154.2)	313 (154.2)	39 (19.2)
20 (511.56)	5000 (2558)	>5000 (>2558)	5000 (2558)	1250 (639.5)	313 (160.1)	313 (160.1)	313 (160.1)

two. On the contrary, compounds **2**, **7** and **20** appear to be the worst performing chelators of this series. Interestingly, compound **10** performs poorly against *E. coli* but very well against *C. albicans*. If the efficacy of the chelators was simply linked to the thermodynamics of their Fe^{3+} chelation (e.g. pFe^{3+}), one could expect to observe the same rank ordering across the microorganism panel, the interspecies variations in MIC being indicative of the capacity of each microbe to deal with the finite competitive challenge defined by the chelator dose. The fact that **1**, **3**, **19** appear to be the most effective inhibitors and **2**, **7** and **20** the poorest but that the efficacy of **10** appears variable suggests that strength of metal chelation, if dominant, is not the only factor that influences the measured MIC values. The fact that pFe^{3+} only takes into consideration iron chelation (while bacteria rely on other biologically relevant metals, e.g. Cu^{2+} , Zn^{2+} that can also be chelated more or less efficiently by the added chelators) and does not include kinetics effects (e.g. metallation of the chelator, siderophores and potential transmetallation reactions) may explain these observations.

The chelators' ranking does not appear to be different between Gram-positive and Gram-negative bacteria in the screened set. However, it would appear that the MIC values obtained on the four tested Gram-negative bacteria are higher than on the tested Gram-positive bacteria. It would appear that our strains of *S. aureus* and *C. albicans* were more sensitive to the presence of a chelator than the other microorganisms, up to two orders of magnitude for *S. aureus* (supplementary materials, Table S2). On the contrary the strains of *P. aeruginosa*, *K. pneumoniae* and *E. coli* appear to be the most resistant of all the organisms tested to the presence of the chelators. Both *E. coli* [77,78] and *K. pneumoniae* [79,80] produce enterobactin (**4**), the most powerful known siderophore and therefore they are expected based on thermodynamic considerations to have a high degree of tolerance for added chelators. However, arguably the greatest resistance is exhibited by *P. aeruginosa* which produces the less potent chelators, pyoverdins and pyochelin [81] rather than enterobactin. These siderophores are not expected to thermodynamically compete favourably with chelators such as **3**. Unless in the future it is found that *P. aeruginosa* as suggested displays "still-unexplored uptake capabilities" [12], or secretes powerful (but still unidentified) siderophores, this result would suggest that there are other factors at play than simple thermodynamically competing chelation reactions.

The greater susceptibility of Gram-positive bacteria to added chelator than Gram-negative has already been observed [42] and suggested to be due to the barrier function of Gram-negative outer membrane presented to molecules of this size (molar masses in Table 1). However, we argue here that the chelators' contribution to biostasis is likely extracellular, in chelating the metal in the growth medium and therefore that the differential susceptibility of Gram-positive and Gram-negative bacteria is due to other factors. The susceptibility of *B. subtilis* DSM-23,778 to these metal chelators is in contrast to the resilience of two *Bacillus* species (*B. subtilis* and *Benthesicymus cereus*) to 3.4-HOPO-based hexadentate chelators [42]. However, these were wild isolates that

may have had the ability to produce the hexadentate siderophore bacillibactin. It should be noted that *B. subtilis* DSM-23,778 was chosen here for its synthetic limitation to a bidentate siderophore [75] rather than its cellular architecture, so the data presented here should not be considered in arguments surrounding efficacy and the possession of an outer membrane. Furthermore, the size and composition of the microbial panels tested here and elsewhere [42] are limited and such mechanistic detail will require careful design of more extensive experiments than were appropriate in this preliminary study.

As the siderophores produced by each of these bacterial strains have not all been formally identified and/or their Fe^{3+} binding efficacy measured, it is not yet possible to determine with a high level of confidence whether the bacteria most resistant to external chelators are systematically the ones that produce the strongest siderophores (highest pFe^{3+}). Also, for each siderophore, its pFe^{3+} is influenced by its total concentration and these can vary over time and as a function of the ability of the microorganism to excrete them in large quantity.

The poor range of hexadentate chelators based on 1.2-HOPO described in the literature needs to be addressed if these are to be seriously considered in therapeutic applications. Consideration of the high efficacy of chelator **19**, where the HOPO group is linked to the TACN core via a methylene group, and the poor efficacy of **7**, where the linker is a carbonyl, suggests that optimisation of the linker will be critical. Comparison of chelators **1**, **7** and **19** suggest that the use of a more rigid macrocyclic scaffold compared to the tris(2-aminoethyl)amine core (to promote chelation via entropic effects) was not successful in improving biological activity.

All the HOPO-based chelators tested herein were designed with the goal of optimising Fe^{3+} chelation. This does not mean that trapping of other essential metals is not concomitantly achieved that leads to the biostatic effect. The amount of key metals in the growth medium was measured and found to be 65.7 μM for iron, 31.5 μM for zinc, 13.7 μM for manganese, 8.3 μM for cobalt and 4.5 μM for copper. For all the microorganisms tested except *C. albicans*, the MIC is above the concentration of iron, as would be expected if our hypothesised mechanism of action is valid. However, the MIC observed on *C. albicans* of 39 μM for **3**, **10** and **19** suggests either that partial chelation of iron is enough to have a biostatic effect on that microorganism or that our chelator also targets other metals that have a much more dramatic effect on its growth or that it affects the organism in a manner not related to metal limitation.

Finally, the effect of added chelators on the availability of other biologically important metals must also be taken into consideration as discussed above. It is therefore unwise to try and rationalise the data presented herein based on relative pFe^{3+} values. Progress towards an understanding of their mode of action however can be made by considering the siderophores that are known to be produced by the tested organisms. Further work is in progress to investigate in depth the mechanism of action of these chelators and to correlate their activity to the thermodynamics and kinetics of their metal binding.

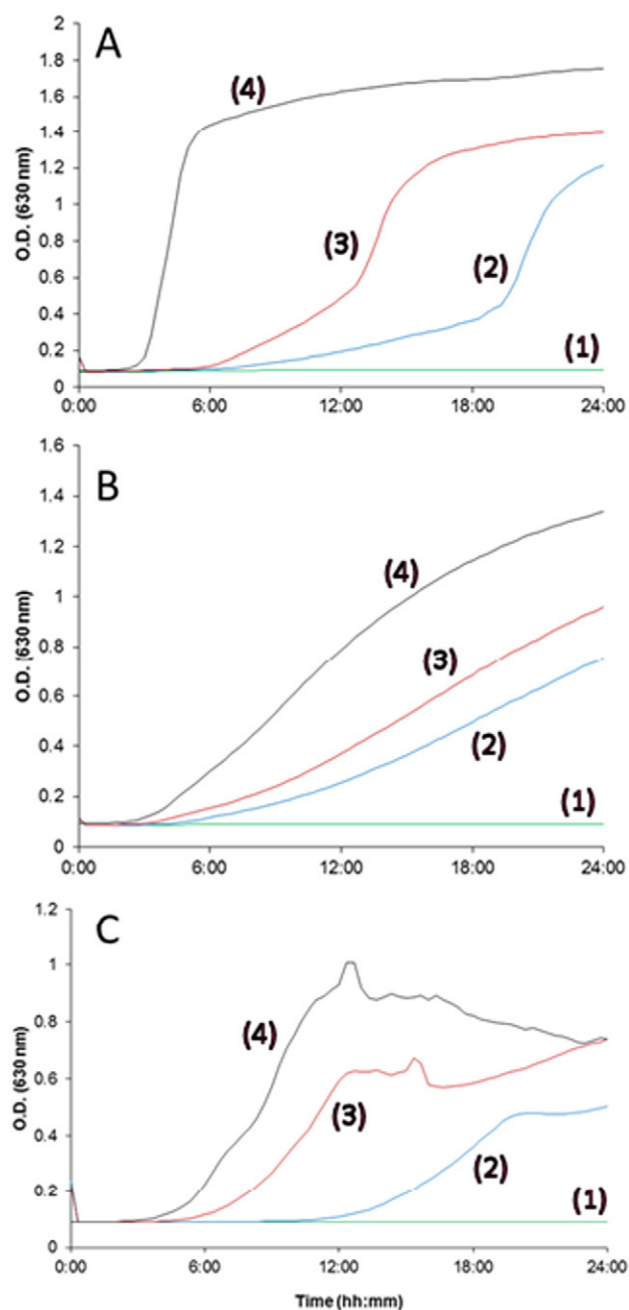


Fig. 6. Impact of sub MIC concentrations on growth of selected bacteria. Panel A describes *K. pneumoniae* DSM-30,104 grown with 3; Panels B and C describe, *P. aeruginosa* DSM-19,880 (B) and *A. baumannii* DSM-30,007 (C) both grown with 19. In each case, MIC (green, (1)) and two sub-MIC concentrations were followed: MIC/4 (red, (3)), MIC/2 (blue, (2)), and the untreated control (black, (4)). Readings were taken every 20 min.

The impact of sub-MIC concentrations on the growth of the microorganisms was followed by optical density (Fig. 6).

As expected each microorganism in the absence of the added chelator, shows a lag phase before entering exponential growth. In the presence of the added chelator, the lag phase appears longer in some cases (e.g. *K. pneumoniae* + 3 at MIC/4) but is not substantially increased in the other cases tested, although a decrease in growth rate is evident. In all the tested cases and by definition, the lag phase was over 24 h when the chelator was used at the MIC value derived from the previous assays. What is apparent for all tested combination is that the rate of

growth is significantly reduced with increasing concentrations of chelators. These growth profiles are consistent with the expected mode of action of the chelators. The microorganisms that suffer from the biostatic effect of a metal chelator find themselves in iron deprivation conditions due to the presence of the said chelator. They therefore have to produce a large amount of siderophore to compete and only when the chelator's pFe^{3+} is overcome by the siderophore's pFe^{3+} value will any growth be initiated. The higher the amount of chelator, the longer it takes the microorganisms to overcome the effect of the biostatic agent. This is consistent with the hypothesis the compounds operate as an extracellular chelator.

3. Conclusion

We report the synthesis of a range of hexadentate chelators based on triaza macrocycles, including the first report of the use of a methylene as a linker between a 1,2-HOPO coordinating group and the molecular scaffold. The ligands have a demonstrable biostatic effect upon the growth of a range of microbes. It is suggested that metal chelation is the main mode of action of these chelators but that a simple thermodynamic competition between the chelator and bacterial siderophore for Fe^{3+} is too simple a picture. Further work is in progress to understand the mode of action of these chelators in detail and to synthesise a wider range of hexadentate chelators based on 1,2-HOPO to assess their efficacy as biostatic agents. These compounds will also form the basis for the study of the effect of the linker between the 1,2-HOPO moiety and the molecular backbone on the thermodynamic efficacy of Fe^{3+} chelation via measurements of pK_a and β_{110} values.

4. Experimental

4.1. Preparation of stock solutions

Glassware was rinsed with a deionised aqueous solution of EDTA (0.1 M) then rinsed thoroughly with deionised water (18 mΩ) before ligands were dissolved in deionised water to the desired concentration (5 mM; 5 mL). The stock solution was then passed through a membrane filter (0.22 μm) into a sterile bijoux tube (7 mL) and stored at 4 °C until required.

4.2. Bacterial strains

All strains were purchased from DSMZ. *E. coli* DSM-18,039, *K. pneumoniae* DSM-30,104, *P. aeruginosa* DSM-19,880 and *S. aureus* DSM-1104 were cultured onto brain heart infusion (BHI) agar and incubated at 37 °C for 24 h. Similar procedures were conducted for strains of *A. baumannii* DSM-30,007 and *C. albicans* DSM-1386 incubated at 30 °C and *B. subtilis* incubated at 25 °C, all for 48 h. The cultured plates were then stored at 4 °C until needed.

4.3. Antimicrobial assay

The assay conducted was based upon a similar literature procedure [76]. Stock solutions of ligands (5000 μM) were added to the first wells of a 96 well-microtitre plate (200 μL) and sterile BHI broth (100 μL) was added to the remaining wells in the row. Ligand solution from the first well (100 μL) was added to the next well in the row and mixed. The procedure was then repeated along the row from the dilute solutions and discarded after the penultimate well. Inoculum (10⁵ CFU/mL; 100 μL) was then added to all wells and the plate incubated without agitation at 37 °C. Readings were taken after 24 and 48 h, depending upon the microorganism, and the MIC determined on the basis of visual turbidity of the well. Assays were performed in triplicate.

4.4. Organic synthesis

All solvents and reagents were purchased from Sigma-Aldrich, Acros Organics or Alfa-Aesar and used without further purification unless otherwise specified. Reactions were followed by TLC using silica gel with UV₂₅₄ fluorescent indicator and column chromatography was conducted using 0.060–0.20 mm silica gel (70–230 mesh), where automated flash column chromatography was conducted using a Biotage Isolera One ISO1SV. Hydrogenations performed using an H-cube® continuous flow hydrogen generator was operated as specified.

4.5. Physical measurements

Melting points were taken on a SRS DigiMelt MPA161 digital melting point apparatus with samples prepared in SAMCO soda glass capillary tubes 100 mm. NMR spectra were recorded using a Jeol JNM Ex270 instrument at 270 MHz and 68 MHz or a Jeol JNM-ECS400 instrument at 400 MHz and 100 MHz, as specified, for ¹H and ¹³C NMR respectively, and are reported in ppm (δ). Infrared spectra were obtained using Durascope diamond ATR system on a Perkin Elmer RX1 FTIR spectrometer. Positive and negative electrospray ionisation mass spectrometry (ESI-MS) was conducted using a Thermo LCQ Advantage mass spectrometer by direct injection. High resolution mass spectrometry were obtained in a Finnigan MAT900XLT high-resolution double focussing mass spectrometer using nano-electrospray ionisation (NESI) at the EPSRC National Mass Spectrometry Service (University of Swansea, Wales, UK). UV–Visible spectrophotometry was conducted using a Varian Cary 50 UV–vis spectrophotometer (range 200–800 nm) using a 1 cm quartz cell at room temperature (18–22 °C). Optical density readings were taken using a Biotek HT Multi-mode Microplate reader at the wavelength specified. Compounds **1** [49], **2** [48], **3** [67] and **8** [60] were synthesised as described. TACN was synthesised using the Richman-Atkins method with slight modification [82,83]. TACD was prepared via modification to the methodology developed by Alder et al. [84,85].

4.5.1. 1-Hydroxy-6-oxo-1.6-dihydropyridine-2-carboxylic acid (**13**)

Using a modified version of a literature method [60], to a suspension of 6-hydroxypicolinic acid **12** (26.20 g, 188 mmol) in glacial acetic acid (160 mL) was carefully added peroxyacetic acid (36–40%, 80 mL). The temperature was carefully raised to 80 °C and stirring was continued for 12 h. The flask was allowed to cool to room temperature and the resulting solid precipitate was collected by filtration and washed with diethyl ether, affording the title compound **13** as a cream solid (18.17 g, 77%). Mp 223–226 °C (from AcOH, Lit [64], 216 °C). $v_{\max}(\text{neat})/\text{cm}^{-1}$ 3114 (O–H), 1611 (CO), 1505 (CO), 1198. $\delta_{\text{H}}(399.8 \text{ MHz, DMSO-}d_6)$ 6.65 (1H, dd, *J* 7.3, 1.8, 3-H), 6.73 (1H, dd, *J* 9.2, 1.8, 5-H), 7.46 (1H, dd, *J* 8.7, 6.9, 4-H). $\delta_{\text{C}}(100.5 \text{ MHz, DMSO-}d_6)$ 106.8 (ArC), 120.8 (ArC), 137.3 (ArC), 139.5 (quat), 157.7 (quat), 162.4 (quat).

4.5.2. Methyl 1-hydroxy-6-oxo-1.6-dihydropyridine-2-carboxylate (**14**) [64]

To a suspension of acid **13** (15.73 g, 101 mmol) in methanol (200 mL) at 0 °C was added thionyl chloride (31.00 g, 426 mmol) dropwise. The mixture was heated under reflux for 4 h. The solution was then allowed to cool to room temperature and the solvent was removed in vacuo to afford the title compound **14** as a cream solid (16.47 g, 96%). Mp 106–108 °C (from MeOH, Lit [64], 90–92 °C). $v_{\max}(\text{neat})/\text{cm}^{-1}$ 3115 (O–H), 1732 (CO), 1505 (CO), 1204. $\delta_{\text{H}}(399.8 \text{ MHz, DMSO-}d_6)$ 3.87 (3H, s, CO₂CH₃), 6.53 (1H, dd, *J* 6.9, 1.4, 3-H), 6.69 (1H, dd, *J* 9.2, 1.4, 5-H), 7.45 (1H, dd, *J* 9.2, 6.9, 4-H). $\delta_{\text{C}}(100.5 \text{ MHz, DMSO-}d_6)$ 53.8 (CO₂CH₃), 105.8 (ArC), 122.6 (ArC), 137.8 (ArC), 138.8 (quat), 158.1 (quat), 161.4 (quat).

4.5.3. Methyl 6-oxo-1-(allyloxy)-1.6-dihydropyridine-2-carboxylate (**15**)

To a solution of compound **14** (16.47 g, 97 mmol) in acetonitrile (200 mL) was added potassium carbonate (32.11 g, 232 mmol), followed by allyl bromide (28.10 g, 232 mmol). The flask was heated under reflux for 4 h before the reaction mixture was filtered and the solvent removed under high vacuum. The residue was dissolved in toluene (100 mL) and the solvent was evaporated in vacuo to afford the title compound **15** as a white crystalline solid (19.12 g, 94%). Mp 65–67 °C (from toluene). Found C, 57.06; H, 5.38; N, 6.67%; C₁₀H₁₁NO₄ requires C, 57.41; H, 5.30; N, 6.70%. $v_{\max}(\text{neat})/\text{cm}^{-1}$ 3462, 3078, 2953, 1735 (CO), 1661 (CO), 1586 (CC), 1445, 1275, 1209, 1136. $\delta_{\text{H}}(399.8 \text{ MHz, DMSO-}d_6)$ 3.94 (3H, s, CO₂CH₃), 4.90 (2H, d, *J* 6.9, CH₂CHCH₂), 5.42 (2H, m, CH₂CHCH₂), 6.08 (1H, m, CH₂CHCH₂), 6.53 (1H, dd, *J* 6.9, 1.8, 3-H), 6.80 (1H, dd, *J* 9.2, 1.8, 5-H), 7.31 (1H, dd, *J* 9.6, 6.9, 4-H). $\delta_{\text{C}}(100.5 \text{ MHz, DMSO-}d_6)$ 53.3 (CH₂CHCH₂), 78.1 (CO₂CH₃), 107.9 (CH₂CHCH₂), 121.9 (CH₂CHCH₂), 126.0 (ArC), 130.6 (ArC), 137.2 (ArC), 138.7 (quat), 158.8 (quat), 160.6 (quat). *m/z* (NESI) 210.0759 ([M + H]⁺); C₁₀H₁₂NO₄ requires 210.0766.

4.5.4. 6-(Hydroxymethyl)-1-(allyloxy)pyridin-2(1H)-one (**16**)

To a suspension of compound **15** (19.12 g, 92 mmol) in THF (200 mL) was added solid sodium borohydride (25.07 g, 663 mmol) in small portions. The solution was heated under reflux for 15 min. Methanol (14 mL) was then added dropwise at reflux over 2 h. The solution was then cooled to 0 °C, quenched by careful addition of saturated aqueous ammonium chloride (25 mL) and stirring was continued for 15 min. The solvents were removed in vacuo and the residue was extracted with dichloromethane (3 × 25 mL). The combined organic extracts were dried and evaporated to afford the title compound **16** as an off-white solid (10.83 g, 65%). Mp 101–104 °C (from DCM). Found C, 59.23; H, 6.23; N, 7.59%; C₉H₁₁NO₃ requires C, 59.66; H, 6.12; N, 7.73%. $v_{\max}(\text{neat})/\text{cm}^{-1}$ 3198 (O–H), 2896, 2842, 1650 (CO), 1560 (CC), 1441, 1154, 1093. $\delta_{\text{H}}(399.8 \text{ MHz, CDCl}_3, \text{Me}_4\text{Si})$ 2.74 (1H, t, *J* 6.4, CH₂OH), 4.68 (2H, d, *J* 6.4, CH₂OH), 4.84 (2H, d, *J* 6.4, CH₂CHCH₂), 5.43 (2H, m, CH₂CHCH₂), 6.06 (1H, m, CH₂CHCH₂), 6.24 (1H, d, *J* 6.9, 3-H), 6.50 (1H, dd, *J* 9.2, 1.4, 5-H), 7.30 (1H, dd, *J* 9.2, 6.9 4-H). $\delta_{\text{C}}(100.5 \text{ MHz, CDCl}_3, \text{Me}_4\text{Si})$ 59.4 (CH₂CHCH₂), 103.7 (CH₂CHCH₂), 120.4 (CH₂CHCH₂), 122.6 (ArC), 130.3 (ArC), 138.7 (ArC), 148.9 (quat), 159.7 (quat). *m/z* (NESI) 182.0811 ([M + H]⁺); C₉H₁₂NO₃ requires 182.0817.

4.5.5. *N,N',N''*-tris(1-benzyloxy-6(1H)-pyridinone-2-carbonyl)-1,4,7-triazacyclononane (**9**)

Following a reported procedure [60] a solution of TACN (0.21 g; 1.6 mmol) and **8** (1.42 g, 8.2 mmol) in dry tetrahydrofuran (40 mL) was added triethylamine (0.55 g, 5.4 mmol) and stirred at 60 °C for 16 h after which the mixture was concentrated to dryness in vacuo. The residue was then partitioned between water (50 mL) and dichloromethane (50 mL) and the organic layer washed with aqueous hydrochloric acid (1 M; 50 mL), aqueous sodium hydroxide (1 M; 50 mL) and brine (50 mL). The organic layer was then dried using magnesium sulfate and filtered before solvent removal in vacuo. Purification of the resulting residue by automated flash chromatography (dichloromethane: methanol, 0–10%) yielded the product as a white solid (0.36 g, 25%); mp 164–170 °C. $\delta_{\text{H}}(400 \text{ MHz; CDCl}_3, \text{Me}_4\text{Si})$ 2.07–4.26 (12H, mm) 4.81 (1H, d, *J* 8.2 Hz) 4.87 (1H, d, *J* 8.7 Hz) 5.04 (1H, m) 5.49–6.06 (5H, mm) 6.68–6.89 (7H, mm) 7.28–7.60 (16H, m); $\delta_{\text{C}}(100 \text{ MHz})$ 47.9, 48.8, 49.2, 49.8, 77.1, 79.2, 79.7, 80.0, 102.7, 103.3, 123.4, 123.5, 123.6, 128.6, 128.7, 128.8, 129.1, 129.4, 130.1, 130.6, 131.0, 131.3, 132.4, 133.1, 133.8, 137.9, 138.3, 138.4, 140.8, 141.5, 141.9, 157.9, 158.0, 162.9, 163.0, 163.2; (+)-ESI-MS: *m/z* 833.01 (M + Na⁺); NESI: requires; *m/z* 811.3092, found 811.3086 (M + H⁺).

4.5.6. 6-(Chloromethyl)-1-(allyloxy)-2(1H)-pyridinone (**17**)

A solution of **16** (4.88 g, 27 mmol) in dichloromethane (120 mL) was added thionyl chloride (12 mL, 165 mmol) and refluxed for 6 h. Ice

water (100 mL) was added at 0 °C and stirred for 30 min. The phases were then separated and the aqueous phase was extracted with dichloromethane (2 × 100 mL). The combined organic phases were dried using magnesium sulfate, filtered and solvent removed in vacuo, yielding a brown oil which solidified upon standing (4.95 g, 92%); mp 62–65 °C. δ_{H} (400 MHz; CDCl₃; Me₄Si) 4.57 (2H, s) 4.93 (2H, d, *J* 6.7 Hz) 5.47 (2H, m) 6.12 (1H, m) 6.25 (1H, dd, *J* 1.7, 6.7 Hz) 6.68 (1H, dd, *J* 1.7, 9.2 Hz) 7.27 (1H, dd, *J* 7.0, 9.4 Hz); δ_{C} (100 MHz) 39.5, 77.5106.4, 122.5, 123.1, 130.3, 137.8, 144.3, 159.3; NESI: requires; *m/z* 200.0478, found; 200.0472 (M⁺).

4.5.7. *N,N',N''-tris(1-hydroxy-6(1H)-pyridinone-2-carbonyl)-1,4,7-triazacyclononane (7)*

A solution of **9** (0.358 g, 0.44 mmol) in a concentrated hydrochloric acid: glacial acetic acid mixture (1: 1; 12 mL) was stirred for 4 days at room temperature then for 2 days at 50 °C. Solvent removal in vacuo yielded a white solid foam (0.230 g, 97%); mp >260 °C. δ_{H} (400 MHz; [D₆]-DMSO; Me₄Si) 3.03–3.82 (12H, m) 6.12–6.35 (2H, m) 6.37–6.63 (4H, m) 7.11 & 7.23 (1H, m) 7.29–7.48 (4H, m); δ_{C} (100 MHz) 48.4–49.6 (m), 103.1 (m), 120.1, 138.4 (m), 141.7, 157.8–158.0, 163.3; (+)-ESI-MS: *m/z* 541.13 (M + H⁺) 563.10 (M + Na⁺); NESI: requires; *m/z* 563.1502, 541.1683, found; 563.1490 (M + Na⁺) 541.1672 (M + H⁺).

4.5.8. *N,N',N''-tris(1-allyloxy-6(1H)-pyridinone-2-methyl)-1,4,7-triazacyclononane (18)*

A mixture of **17** (0.448 g, 2.24 mmol), potassium carbonate (0.41 g, 3.0 mmol) and TACN (0.095 g, 0.74 mmol) in acetonitrile (20 mL) was refluxed overnight. The mixture was then added to water (50 mL) before extraction with dichloromethane (3 × 50 mL). The organic extracts were washed with brine (50 mL) before being dried with magnesium sulfate and the solvent removed in vacuo to yield a dark orange highly viscous liquid (0.431 g, 93%). δ_{H} (400 MHz; CDCl₃; Me₄Si) 2.87 (12H, s) 3.72 (6H, s) 4.79 (6H, d, *J* 6.4 Hz) 5.38 (6H, m) 6.05 (3H, m) 6.15 (3H, dd, *J* 1.4, 6.9 Hz) 6.56 (3H, dd, *J* 1.4, 9.2 Hz) 7.24 (3H, dd, *J* 6.9, 9.2 Hz); δ_{C} (100 MHz) 55.9, 57.1, 76.7, 104.8, 120.4, 122.1, 130.5, 137.9, 147.7, 159.7; (+)-ESI-MS: *m/z* 619.05 (M + H⁺); NESI: requires; *m/z* 619.3244, found; 619.3243 (M + H⁺).

4.5.9. *N,N',N''-tris(1-hydroxy-6(1H)-pyridinone-2-methyl)-1,4,7-triazacyclononane. 3 HCl (19)*

Under an atmosphere of nitrogen, a solution of **18** (0.759 g, 1.2 mmol) in dry dichloromethane (8 mL) at 0 °C was added boron trichloride in hexane (1.0 M; 8.6 mL, 8.6 mmol) and vigorously stirred overnight before the mixture was added methanol (8 mL) and stirred for 30 min further. The solution was then evaporated in vacuo and re-evaporated with methanol (10 mL) 5 times, yielding the crude as brown flakes. Dissolution in a minimum volume of methanol and precipitation using diethyl ether yielded a cream solid following collection by Büchner filtration and washing with diethyl ether (0.534 g, 87%), mp 180 °C (decomp.). δ_{H} (400 MHz; [D₆]-DMSO; Me₄Si) 3.01 (12H, s) 4.18 (6H, s) 6.34 (3H, dd, *J* 1.4, 6.9 Hz) 6.54 (3H, dd, *J* 1.4, 9.2 Hz) 7.39 (3H, dd, *J* 6.9, 9.2 Hz); δ_{C} (100 MHz) 49.3, 53.1, 106.8, 118.5, 137.5, 141.9, 158.5.

4.5.10. *N,N',N''-tris(1-benzyloxy-6(1H)-pyridinone-2-carbonyl)-1,5,9-triazacyclododecane (11)*

Product was prepared based upon a similar literature procedure [60]. To a solution of TACD (0.18 g; 1.1 mmol) and triethylamine (0.46 g, 4.5 mmol) in dry *N,N*-dimethylformamide (5 mL) was added **8** (0.89 g, 3.4 mmol) and was stirred at 60 °C in a stoppered flask for 48 h. After this time the mixture was concentrated to dryness in vacuo and the residue was dissolved in dichloromethane (50 mL) before being washed with aqueous hydrochloric acid (1 M; 50 mL), aqueous sodium hydroxide (1 M; 50 mL), water (3 × 50 mL) and brine (50 mL). The organic layer was then dried using magnesium sulfate and filtered before solvent removal in vacuo. Purification of the

resulting residue by automated flash chromatography (dichloromethane: methanol, 1–6%) yielded the product as a white solid (0.44 g, 49%); mp 118–123 °C. δ_{H} (400 MHz; CDCl₃; Me₄Si) 0.89–3.94 (18H, mm) 4.83–5.04 (3H, mm) 5.38–6.04 (5H, mm) 6.64–7.18 (4H, mm) 7.25–7.58 (18H, mm); δ_{C} (100 MHz; CDCl₃; Me₄Si) 24.5, 25.5, 25.9, 26.6, 27.0, 28.8, 31.4, 36.5, 42.2, 44.6, 45.7, 45.8, 46.3, 46.6, 46.8, 48.5, 49.2, 79.3, 79.4, 79.5, 79.7, 102.2, 102.3, 102.5, 102.6, 102.7, 123.0, 123.1, 123.2, 123.3, 123.4, 128.4, 128.5, 128.7, 128.8, 129.0, 129.2, 129.4, 129.5, 129.7, 129.9, 130.0, 130.0, 130.2, 130.3, 130.5, 130.7, 130.7, 131.3, 133.1, 133.4, 133.5, 133.6, 133.7, 133.8, 137.2, 138.0, 138.0, 138.1, 138.2, 138.3, 138.4, 138.5, 138.5, 141.9, 142.2, 142.3142.4, 142.6, 142.6, 142.6, 142.7, 158.0, 158.1, 158.1, 158.2, 158.2, 161.9, 162.0, 162.1, 162.4, 162.5, 163.0; (+)-ESI-MS: *m/z* 875.16 (M + H⁺); NESI: requires; *m/z* 875.3380, 853.3561; found; 875.3366 (M + Na⁺) 853.3555 (M + H⁺).

4.5.11. *N,N',N''-tris(1-benzyloxy-6(1H)-pyridinone-2-carbonyl)-1,5,9-triazacyclododecane (10)*

A solution of **11** (0.268 g, 4.3 mmol) in a mixture of concentrated hydrochloric acid and glacial acetic acid (1: 1; 12 mL) was stirred at ambient temperature for 4 days before stirring overnight at 50 °C. The solution was then concentrated to dryness in vacuo before dissolution in a minimum volume of methanol and solid precipitation by diethyl ether addition. The product was collected by Büchner filtration and washed with diethyl ether yielding a white powder (0.130 g, 71%); mp 161–169 °C. δ_{H} (400 MHz; [D₆]-DMSO; Me₄Si) 1.78–2.15 (6H, m, br) 2.96–3.52 (12H, m, br) 6.17–6.34 (3H, m, br) 6.49–6.59 (3H, m) 7.32–7.47 (3H, m); δ_{C} (100 MHz) 42.7, 43.4, 46.5, 47.6, 82.9, 102.0, 119.0, 137.5, 137.6, 137.6, 141.5, 141.6, 141.6, 157.2, 157.2, 161.8, 162.1; (–)-ESI-MS: *m/z* 581.16 ([M – H][–]), HRMS NESN: requires; 581.1996, found; 581.1985 ([M – H][–]).

4.5.12. *N,N',N''-tris(1-benzyloxy-6(1H)-pyridinone-2-carbonyl)-bis(2-aminoethyl)amine (21)*

Product was prepared based upon a similar literature procedure [60]. A mixture of **8** (1.29 g, 4.9 mmol) and triethylamine (1.35 g, 13.3 mmol) in dry tetrahydrofuran (20 mL) was added diethylenetriamine (0.15 g, 1.5 mmol) and stirred in a stoppered flask overnight at 60 °C. The mixture was then concentrated to dryness in vacuo and the residue dissolved in a mixture of water (100 mL) and dichloromethane (100 mL). Separation of the phases and washing of the organic layer with aqueous sodium hydroxide (1 M; 100 mL), aqueous hydrochloric acid (1 M; 100 mL) then brine (100 mL) before drying over magnesium sulfate, filtration and solvent removal in vacuo yielded the crude residue which was purified by automated flash chromatography (dichloromethane: methanol, 1–11%) yielding the product as a hygroscopic solid (1.04 g, 91%); mp 84–89 °C. δ_{H} (400 MHz; CDCl₃; Me₄Si) 3.04–3.28 (6H, m) 3.48 (1H, d, *J* 4.1 Hz) 3.84 (1H, m) 4.94 (1H, d, *J* 7.8 Hz) 5.21 (1H, d, *J* 8.7 Hz) 5.29–5.40 (4H, m) 5.63 (1H, d, *J* 7.8 Hz) 6.03 (1H, dd, *J* 1.8, 6.9 Hz) 6.14 (1H, dd, *J* 1.4, 6.9 Hz) 6.19 (1H, dd, *J* 1.4, 6.9 Hz) 6.60 (1H, dd, *J* 1.4, 9.2 Hz) 6.65 (1H, t, *J* 5.5 Hz) 6.71 (1H, dd, *J* 1.4, 9.2 Hz) 7.17 (1H, dd, *J* 6.4, 9.2 Hz) 7.22 (1H, dd, *J* 6.4, 9.2 Hz) 7.25 (1H, dd, *J* 6.4, 9.2 Hz) 7.30–7.33 (10H, m) 7.41–7.44 (4H, m) 7.49–7.52 (2H, m); δ_{C} (100 MHz) 38.2, 45.8, 48.5, 79.2, 79.3, 79.4, 103.1, 105.6, 105.9, 123.3, 124.5, 124.7, 128.7, 128.7, 129.5, 129.6, 129.7, 130.1, 130.4, 130.5, 133.2, 133.3, 133.5, 137.9, 137.9, 138.4, 141.9, 141.9, 142.0, 145.6, 158.0, 158.4, 160.7, 161.0, 163.0; (+)-ESI-MS: *m/z* 807.02 (M + Na⁺); NESI: requires; *m/z* 785.2935, found; 785.3272 (M + H⁺).

4.5.13. *N,N',N''-tris(1-hydroxy-6(1H)-pyridinone-2-carbonyl)-bis(2-aminoethyl)amine (20)*

A solution of **21** (0.35 g, 0.46 mmol) in a mixture of concentrated hydrochloric acid and glacial acetic acid (1: 1; 12 mL) was stirred at room temperature for 4 days before solvent removal in vacuo. The crude solid was then dissolved in a minimum volume of methanol and precipitated

by addition of diethyl ether, yielding an off-white powder collected by Büchner filtration (0.16 g, 70%). δ_{H} (400 MHz; [D₆]-DMSO; Me₄Si) 3.37 (4H, s, br) 3.48 (4H, s, br) 6.28 (3H, m) 6.56 (2H, m) 7.33–7.39 (3H, m) 8.85 (1H, t, br) 8.93 (1H, t, br); δ_{C} (100 MHz) 37.0, 37.8, 44.5, 47.8, 102.9, 104.3, 104.6, 119.8, 120.1, 137.7, 137.9, 138.3, 142.0, 142.3, 142.6, 157.9, 158.0, 160.9, 161.1, 162.4, 162.9, 172.6; (+)-ESI-MS: m/z 537.09 (M + Na⁺); HRMS NESN: requires; m/z 513.1370, found; 513.1376 (M – H)[–].

Acknowledgements

The authors are grateful for financial support from the Healthcare Infection Society (www.his.org.uk) and Northumbria University. The authors are also grateful for the support offered by the EPSRC National Mass Spectrometry Service (Swansea, Wales, UK) for high resolution mass spectrometry. Dr Frank Lewis (Northumbria University), Dr Valery Kozhevnikov (Northumbria University) and Dr Jon Bookham (Northumbria University) are also acknowledged for fruitful discussions. We are indebted to a reviewer for suggesting conducting the Ga³⁺ 1H NMR experiments to improve the quality of the manuscript.

Appendix A. Supplementary data

Supplementary data to this article can be found online at <http://dx.doi.org/10.1016/j.jinorgbio.2016.04.018>.

References

- [1] J. Davies, D. Davies, *Microbiol. Mol. Biol. Rev.* 74 (2010) 417–433.
- [2] C.A. Arias, B.E. Murray, *New Engl. J. Med.* 360 (2009) 439.
- [3] G.J. Kontoghiorghes, A. Kolnagou, A. Skiada, G. Petrikos, *Hemoglobin* 34 (2010) 227–239.
- [4] E. Banin, K.M. Brady, E.P. Greenberg, *Appl. Environ. Microbiol.* 72 (2006) 2064–2069.
- [5] R.J.W. Lambert, G.W. Hanlon, S.P. Denyer, *J. Appl. Microbiol.* 96 (2004) 244–253.
- [6] S.H. Hartzen, N. Frimodt-Møller, V.F. Thomsen, *Acta Pathol. Microbiol. Immunol. Scand.* 99 (1991) 879–886.
- [7] B.S. van Asbeck, J.H. Marcelis, J.H. van Kats, E.Y. Jaarsma, J. Verhoef, *Eur. J. Clin. Microbiol.* 2 (1983) 432–438.
- [8] T.L. Foley, A. Simeonov, *Expert Opin. Drug Discovery* 7 (2012) 831–847.
- [9] B.D. Corbin, E.H. Seeley, A. Raab, J. Feldmann, M.R. Miller, V.J. Torres, K.L. Anderson, B.M. Dattilo, P.M. Dunman, R. Gerads, R.M. Caprioli, W. Nacken, W.J. Chazin, E.P. Skaar, *Science* 319 (2008) 962–965.
- [10] Y. Zhang, C. Eric Ballard, S.L. Zheng, X. Gao, K.C. Ko, H. Yang, G. Brandt, X. Lou, P.C. Tai, C.D. Lu, B. Wang, *Bioorg. Med. Chem. Lett.* 17 (2007) 707–711.
- [11] P.T. Lieu, M. Heiskala, P.A. Peterson, *Y. Yang, Mol. Asp. Med.* 22 (2001) 1–87.
- [12] P. Visca, C. Bonchi, F. Minandri, E. Frangipani, F. Imperi, *Antimicrob. Agents Chemother.* 57 (2013) 2432–2433.
- [13] L. de Léséleuc, G. Harris, R. Kuolee, W. Chen, *Antimicrob. Agents Chemother.* 56 (2012) 5397–5400.
- [14] M.G. Thompson, B.W. Corey, Y. Si, D.W. Craft, D.V. Zurawski, *Antimicrob. Agents Chemother.* 56 (2012) 5419–5421.
- [15] A.S. Ibrahim, T. Gebermariam, Y. Fu, L. Lin, M.I. Hussein, S.W. French, J. Schwartz, C.D. Skory, J.E. Edwards Jr., B.J. Spellberg, *J. Clin. Invest.* 117 (2007) 2649–2657.
- [16] M. Nairz, A. Schroll, T. Sonnweber, G. Weiss, *Cell. Microbiol.* 12 (2010) 1691–1702.
- [17] C. Ratledge, *Food Nutr. Bull.* 28 (2007) S515–S523.
- [18] C. Ratledge, L.G. Dover, *Annu. Rev. Microbiol.* 54 (2000) 881–941.
- [19] S.C. Andrews, A.K. Robinson, F. Rodriguez-Quinones, *FEMS Microbiol. Rev.* 27 (2003) 215–237.
- [20] R.C. Hider, X. Kong, *Nat. Prod. Rep.* 27 (2010) 637–657.
- [21] K.D. Krewulak, H.J. Vogel, *Biochim. Biophys. Acta* 1778 (2008) 1781–1804.
- [22] M. Miethke, M.A. Marahiel, *Microbiol. Mol. Biol. Rev.* 71 (2007) 413–451.
- [23] H. Boukhalifa, A.L. Crumbliss, *Biomaterials* 15 (2002) 325–339.
- [24] K.N. Raymond, G. Müller, B.F. Matzanke, *Top. Curr. Chem.* 123 (1984) 49–102.
- [25] A.L. Crumbliss, J.M. Harrington, *Adv. Inorg. Chem.* 61 (2009) 179–250.
- [26] Z.D. Liu, R.C. Hider, *Coord. Chem. Rev.* 232 (2002) 151–171.
- [27] A. D'Onofrio, J.M. Crawford, E.J. Stewart, K. Witt, E. Gavriš, S. Epstein, J. Clardy, K. Lewis, *Chem. Biol.* 17 (2010) 254–264.
- [28] R.J. Abergel, M.K. Wilson, J.E. Arceaneux, T.M. Hoette, R.K. Strong, B.R. Byers, K.N. Raymond, *Proc. Natl. Acad. Sci. U. S. A.* 103 (2006) 18499–18503.
- [29] T.H. Flo, K.D. Smith, S. Sato, D.J. Rodriguez, M.A. Holmes, R.K. Strong, S. Akira, A. Aderem, *Nature* 432 (2004) 917–921.
- [30] M.A. Holmes, W. Paulsene, X. Jide, C. Ratledge, R.K. Strong, *Structure* 13 (2005) 29–41.
- [31] D.H. Goetz, M.A. Holmes, N. Borregaard, M.E. Bluhm, K.N. Raymond, *Mol. Cell* 10 (2002) 1033–1043.
- [32] T.M. Hoette, R.J. Abergel, J. Xu, R.K. Strong, K.N. Raymond, *J. Am. Chem. Soc.* 130 (2008) 17584–17592.
- [33] M.A. Santos, *Coord. Chem. Rev.* 252 (2008) 1213–1224.
- [34] M.X. Zhang, C.F. Zhu, Y.J. Zhou, X.L. Kong, R.C. Hider, T. Zhou, *Chem. Biol. Drug Des.* 84 (2014) 659–668.
- [35] Y.J. Zhou, M.S. Liu, A.R. Osamah, X.L. Kong, S. Alsam, S. Battah, Y.Y. Xie, R.C. Hider, T. Zhou, *Eur. J. Med. Chem.* 94 (2015) 8–21.
- [36] Y.J. Zhou, M.X. Zhang, R.C. Hider, T. Zhou, *FEMS Microbiol. Lett.* 355 (2014) 124–130.
- [37] A. Nunes, M. Podinovskaia, A. Leite, P. Gameiro, T. Zhou, Y. Ma, X. Kong, U.E. Schaible, R.C. Hider, M. Rangel, *J. Biol. Inorg. Chem.* 15 (2010) 861–877.
- [38] Y.-J. Zhou, X.-L. Kong, J.-P. Li, Y.-M. Ma, R.C. Hider, T. Zhou, *Med. Chem. Commun.* 6 (2015) 1620–1625.
- [39] Y.-Y. Xie, M.-S. Liu, P.-P. Hu, X.-L. Kong, D.-H. Qiu, J.-L. Xu, R.C. Hider, T. Zhou, *Med. Chem. Res.* 22 (2013) 2351–2359.
- [40] C.F. Zhu, D.H. Qiu, X.L. Kong, R.C. Hider, T. Zhou, *J. Pharm. Pharmacol.* 65 (2013) 512–520.
- [41] B. Xu, X.L. Kong, T. Zhou, D.H. Qiu, Y.L. Chen, M.S. Liu, R.H. Yang, R.C. Hider, *Bioorg. Med. Chem. Lett.* 21 (2011) 6376–6380.
- [42] D.-H. Qiu, Z.-L. Huang, T. Zhou, C. Shen, R.C. Hider, *FEMS Microbiol. Lett.* 314 (2011) 107–111.
- [43] S.S. Fernandes, A. Nunes, A.R. Gomes, B. de Castro, R.C. Hider, M. Rangel, R. Appelberg, M.S. Gomes, *Microbes Infect.* 12 (2010) 287–294.
- [44] L. Deng, J. Diao, P. Chen, V. Pujari, Y. Yao, G. Cheng, D.C. Crick, B.V. Prasad, Y. Song, *J. Med. Chem.* 54 (2011) 4721–4734.
- [45] L. Deng, S. Sundriyal, V. Rubio, Z.Z. Shi, Y. Song, *J. Med. Chem.* 52 (2009) 6539–6542.
- [46] M. Seitz, M.D. Pluth, K.N. Raymond, *Inorg. Chem.* 46 (2007) 351–353.
- [47] D.L. White, P.W. Durbin, N. Jeung, K.N. Raymond, *J. Med. Chem.* 31 (1988) 11–18.
- [48] E.J. Werner, S. Avedano, M. Botta, B.P. Hay, E.G. Moore, S. Aime, K.N. Raymond, *J. Am. Chem. Soc.* 129 (2007) 1870–1871.
- [49] J. Xu, D.G. Churchill, M. Botta, K.N. Raymond, *Inorg. Chem.* 43 (2004) 5492–5494.
- [50] A.E. Martell, R.J. Motekaitis, M.J. Welch, *J. Chem. Soc. Chem. Commun.* (1990) 1748–1749.
- [51] G. Ambrosi, P. Dapporto, M. Formica, V. Fusi, L. Giorgi, A. Guerri, S. Lucarini, M. Micheloni, P. Paoli, R. Pontellini, P. Rossi, G. Zappia, *New J. Chem.* 28 (2004) 1359–1367.
- [52] M. Formica, V. Fusi, L. Giorgi, A. Guerri, S. Lucarini, M. Micheloni, P. Paoli, R. Pontellini, P. Rossi, G. Tarzia, G. Zappia, *New J. Chem.* 27 (2003) 1575–1583.
- [53] Y. Gai, Z. Hu, Z. Rong, X. Ma, G. Xiang, *Molecules* 20 (2015) 19393–19405.
- [54] J.M. Harrington, S. Chittamuru, S. Dhungana, H.K. Jacobs, A.S. Gopalan, A.L. Crumbliss, *Inorg. Chem.* 49 (2010) 8208–8221.
- [55] R.J. Abergel, A.M. Zawadzka, T.M. Hoette, K.N. Raymond, *J. Am. Chem. Soc.* 131 (2009) 12682–12692.
- [56] B.P. Hay, D.A. Dixon, R. Vargas, J. Garza, K.N. Raymond, *Inorg. Chem.* 40 (2001) 3922–3935.
- [57] Z. Hou, T.D.P. Stack, C.J. Sunderland, K.N. Raymond, *Inorg. Chim. Acta* 263 (1997) 341–355.
- [58] R.C. Scarrow, D.J. Ecker, C. Ng, S. Liu, K.N. Raymond, *Inorg. Chem.* 30 (1991) 900–906.
- [59] A. Shanzer, J. Libman, S. Lifson, C.E. Felder, *J. Am. Chem. Soc.* 108 (1986) 7609–7619.
- [60] J. Xu, P.W. Durbin, B. Kullgren, S.N. Ebbe, L.C. Uhler, K.N. Raymond, *J. Med. Chem.* 45 (2002) 3963–3971.
- [61] A.J. Blake, I.A. Fallis, A. Heppeler, S. Parsons, S.A. Ross, M. Schröder, *J. Chem. Soc. Dalton Trans.* (1996) 31–43.
- [62] P.G.M. Wuts, T.W. Greene, *Greene's Protective Groups in Organic Synthesis*, fourth ed. John Wiley & Sons, Inc., 2007.
- [63] D.G. Workman, A. Tsatsanis, F.W. Lewis, J.P. Boyle, M. Mousadoust, N.T. Hettiarachchi, M. Hunter, C. Peers, D. Tétard, J.A. Duce, *Metalomics* 7 (2015) 867–876.
- [64] R. Burgada, T. Bailly, J.P. Noel, J.M. Gomis, A. Valleix, E. Ansoborlo, M.H. Henge-Napoli, F. Paquet, P. Gourmelon, *J. Label. Compd. Radiopharm.* 44 (2001) 13–19.
- [65] N. Boechat, J.C.S. da Costa, J. de Souza Mendonça, P.S.M. de Oliveira, M. Vinícius N. De Souza, *Tetrahedron Lett.* 45 (2004) 6021–6022.
- [66] K. Soai, H. Oyamada, M. Takase, A. Ookawa, *Bull. Chem. Soc. Jpn.* 57 (1984) 1948–1953.
- [67] Y.Z. Sun, A.E. Martell, J.H. Reibenspies, M.J. Welch, *Tetrahedron* 47 (1991) 357–364.
- [68] D.A. Moore, P.E. Fanwick, M.J. Welch, *Inorg. Chem.* 28 (1989) 1504.
- [69] U. Auerbach, U. Eckert, K. Wiegardt, B. Nuber, J. Weiss, *Inorg. Chem.* 29 (1990) 938–944.
- [70] C.-T. Yang, S.G. Sreerama, W.-Y. Hsieh, S. Liu, *Inorg. Chem.* 47 (2008) 2719.
- [71] G. Mohr, P. Koehl, H. Budzikiewicz, J.-F. Lefèvre, *Biochemistry* 33 (1994) 2843.
- [72] M. Seitz, E.G. Moore, K.N. Raymond, *Inorg. Chem.* 47 (2008) 8665–8673.
- [73] S.M. Cohen, K.N. Raymond, *Inorg. Chem.* 39 (2000) 3624–3631.
- [74] L.E. Quadri, P.H. Weinreb, M. Lei, M.M. Nakano, P. Zuber, C.T. Walsh, *Biochemistry* 37 (1998) 1585–1595.
- [75] A. Gaballa, J.D. Helmann, in: C. Pierre, S.C. Andrews (Eds.), *Iron Uptake and Homeostasis in Microorganisms*, Caister Academic Press 2010, pp. 229–246.
- [76] J.M. Andrews, *J. Antimicrob. Chemother.* 48 (Suppl. 1) (2001) 5–16.
- [77] A.M. Gehring, K.A. Bradley, C.T. Walsh, *Biochemistry* 36 (1997) 8495–8503.
- [78] I.G. O'Brien, F. Gibson, *Biochim. Biophys. Acta* 215 (1970) 393–402.
- [79] B. Jaya, C. Sanjay, *Indian J. Med. Microbiol.* 13 (1995) 34–36.
- [80] R.D. Perry, C.L. San Clemente, *J. Bacteriol.* 140 (1979) 1129–1132.
- [81] I.L. Lamont, A.F. Konings, D.W. Reid, *Biomaterials* 22 (2009) 53–60.
- [82] J.Z. Gao, H. He, X. Zhang, X.Q. Lu, J.Q. Kang, *Indian J. Med. Microbiol.* 41 (2002) 372–375.
- [83] J.E. Richman, T.J. Atkins, *J. Am. Chem. Soc.* 96 (1974) 2268–2270.
- [84] R.D. Kim, M. Wilson, J. Haseltine, *Synth. Commun.* 24 (1994) 3109–3114.
- [85] N.J. Long, D.G. Parker, P.R. Speyer, A.J.P. White, D.J. Williams, *J. Chem. Soc. Dalton Trans.* (2002) 2142–2150.